

EUROPHYSICS LETTERS

Europhys. Lett., (), pp. ()

Robust chaos generation by a perceptron

A. Priel() and I. Kanter

Minerva Center and Department of Physics,
Bar-Ilan University, 52900 Ramat-Gan, Israel

(received ; accepted)

PACS.84.35+ i { Neural networks.

PACS.05.45-a { Nonlinear dynamics and nonlinear dynamical systems.

Abstract. { The properties of time series generated by a perceptron with monotonic and non-monotonic transfer function, where the next input vector is determined from past output values, are examined. A analysis of the parameter space reveals the following main finding: a perceptron with a monotonic function can produce fragile chaos only whereas a non-monotonic function can generate robust chaos as well. For non-monotonic functions, the dimension of the attractor can be controlled monotonically by tuning a natural parameter in the model.

Attractor neural networks composed of symmetric interactions were studied using methods closely related to those used in statistical physics for the study of magnetic systems [1]. Chaotic dynamics, however, can occur in asymmetric networks which are more relevant to the structure of biological systems. For instance, analysis of experimental results obtained from EEG recordings revealed chaotic attractors [2], however, the role of this dynamic behavior in the brain is not yet clear. The emergence of chaos in some limited recurrent asymmetric networks was examined either analytically or numerically [3].

Another important class of models with an underlying dynamics which exhibits a chaotic behavior are time-delayed neural networks. These networks are analogous to the non-linear auto-regressive (NAR) models that are widely used for time series analysis. Some of their stationary statistical properties were reviewed by H. Tong [4]. This letter is concerned with noiseless NAR networks where the non-linearity is realized through a feed-forward network. The computational capabilities of such models were found to be equivalent to fully recurrent networks [5]. A similar dynamical system, the generalized shift map, can be viewed as a special case of the noiseless NAR model in which piecewise linear mappings are used. A proposed physical realization of the generalized shift map is demonstrated by the motion of a particle constrained by a system of parabolic mirrors in a 3D billiard [6].

In spite of the advances in the research of these models, the problem of learning a chaotic time series is still an open question and analytical results are hardly available. The interplay, if any, between the details of the network (i.e., its architecture, type of non-linearity and

() Present address: School of Mathematical Sciences, Tel-Aviv University, Tel-Aviv, Israel

parameters) and the characteristics of the chaos generated by the model (e.g., structural stability, attractor dimension) is of both theoretical and practical interest. The simplest NAR network is clearly a perceptron, described mathematically as follows. For a given input vector at time step t , S^t ($S_j^t; j = 1; \dots; N$), the network's output S_{out}^t is given by

$$S_{out}^t = f \left(\sum_{j=1}^N W_j S_j^t \right) \quad (1)$$

where W_j are the weights, θ is a gain parameter and f is a transfer function. The input vector at time $t+1$ is obtained by shifting the previous output values

$$S_1^{t+1} = S_{out}^t; \quad S_j^{t+1} = S_{j-1}^t \quad j = 2; \dots; N \quad (2)$$

This model exhibits (quasi) periodic attractors in the stable regime, regardless of the details of the weights [7]. The same conclusion holds when the network is a multilayer-perceptron (altering eq. 1 accordingly) [8].

One of the main issues that we address in this letter is the interplay between the type of non-linearity and the stability of the chaos generated. In the sequel we present a numerical investigation of the NAR-perceptron using two types of transfer functions: monotonic and non-monotonic. Understanding the behavior of this simple model is essential before turning to the analysis of more complicated architectures. The distinction between monotonic and non-monotonic functions was already pointed out in [9, 10]. Another important question that arises is the capability to control the attractor dimension of the sequence generated by the model. The ability to synthesize a chaotic neural network is clearly a challenging task.

In order to characterize the dynamical properties of the networks, we classify the attractors in phase space in the vicinity of a given vector of parameters while varying some control parameters. In order to minimize the number of free parameters in the model, we represent the weights in the Fourier domain and take only few components. This representation is clearly advantageous in high dimensional systems where varying a large number of parameters is not practical and can not be visualized conveniently. The general prescription of the weights is given by:

$$W_j = \sum_p a_p \cos\left(\frac{2}{N} k_p j + \phi_p\right) + b; \quad j = 1 \dots N; \quad p \in [1:l]; \quad (3)$$

where a_p 's are constant amplitudes; k_p 's are positive integers denoting the wave numbers; ϕ_p 's are the phases; b is the bias term and p runs over the number of Fourier components composing the weights. We investigate only the cases $p = 1$ and 2 , or randomly chosen weights. The analysis of the first question is exemplified by the hyperbolic-tangent function (monotonic) and the sine function (non-monotonic). We emphasize that other functions were tested as well, leading to the same conclusions (e.g., monotonic and non-monotonic piecewise linear functions).

Starting with the monotonic functions, the output, S_{out} , is given by

$$S_{out}^t = \tanh \left(\sum_{j=1}^N W_j S_j^t \right) \quad (4)$$

For weights that consist of a single biased Fourier component we set $a = 1$. In the simplest case of two inputs, $N = 2$, the special case $\phi = 1$ results in the following map

$$S^{t+1} = \tanh \left((1+b)S^t + (1-b)S^{t-1} \right); \quad (5)$$

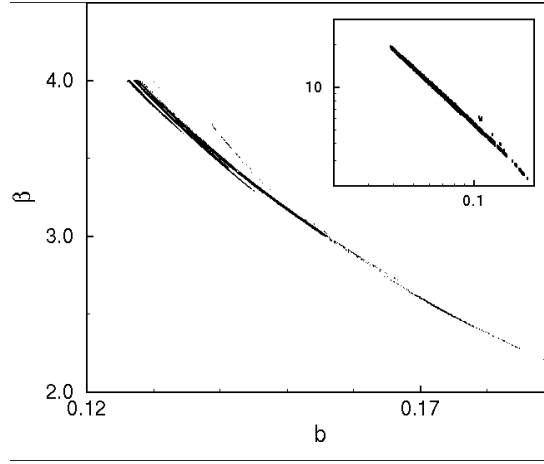


Fig.1. { A region in parameter space for a NAR-perceptron with hyperbolic-tangent transfer function, $N = 3$ and $\theta = 1$ (eq.6), where vector points that lead to chaotic attractors are marked; the remaining space in this region leads to stable attractors. Insert: a (log-log) continuation for higher gain values, indicating a power-law relation $\beta / b^{1.32 \pm 0.001}$.

which is equivalent to a physical model of a magnetic system, the ANNNI model [11]. This map is capable of generating stable attractors (fixed points, periodic and quasi-periodic orbits) as well as unstable chaotic (however, not robust) behavior.

Using the same settings, the map for $N = 3$ is given by:

$$S^{t+1} = \tanh \left((1+2+b)S^t + (1+2+b)S^{t-1} + (1+b)S^{t-2} \right) \quad (6)$$

which is similar to the ANNNI model with competing interactions between third neighbors along the axial direction [12]. In order to analyze numerically the parameter space of the map, it is sampled in a high resolution (up to 10^5). The spectrum of Lyapunov exponents is estimated directly from the dynamic equations using an algorithm described in Wolf et. al. [13] and former authors (references therein). Figure 1 depicts a section of the parameter space of the map given in eq.6. The black dots represent vector points that lead to chaotic behavior with one positive Lyapunov exponent; the remaining space in this region gives rise to stable attractors. Each point has neighboring points which lead to periodic attractors. The insert suggests a possible power-law relation between the gain and the bias terms. The general case $\theta < 1$ can be analyzed in the same manner as that described above. We note that for $N = 2$, no unstable regions are found for $\theta < \frac{1}{2}$.

In higher dimensions (larger N), the parameter space becomes more structured. We demonstrate this behavior for $N = 9$. As before, we restrict the dimension of parameter space to two, $(\theta; b)$, with weights prescribed by:

$$W_j = \cos\left(\frac{2}{N}j + \theta\right) + b; \quad j = 1::N; \quad \theta = 1; \quad N = 9 : \quad (7)$$

Figure 2 depicts a region in parameter space for the case $N = 9$ with $\theta = 1$ (unstable behavior is found outside this region as well). We use $\theta = 1$ here as well since larger phase generates more unstable points. The unstable points span a significant part of the space. Qualitatively, the parameter space is similar to that of $N = 2;3$ in the sense that the chaotic attractors are fragile with a single positive exponent. However, as N increases, the structure of the parameter

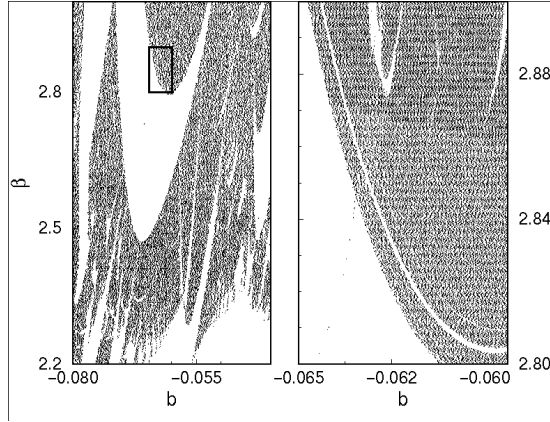


Fig. 2. { Example of a region in parameter space for hyperbolic-tangent transfer function and $N = 9$, where vector points that lead to chaotic attractors are marked; the remaining space in this region leads to stable attractors. The right-hand part is a blow up of the marked rectangle.

space becomes more involved as larger cycles become available. Moreira and Salinas [12] have already mentioned that such a complication is expected at larger N in their model ($N = 3$). We should stress here that the regions of unstable points are not dense; i.e., in the vicinity of every unstable point there exists a stable one, therefore, the chaotic regions are fragile. In particular, these points generate a mixed behavior in phase space; stable and unstable attractors are possible, depending on the initial condition, and both have a non-vanishing basin of attraction. The examples provided so far consist of weights with a single dominant Fourier component in the power spectrum. We tested the case of two Fourier components with bias of the form :

$$W_j = a_1 \cos \left(\frac{2}{N} k_1 j + \phi_1 \right) + a_2 \cos \left(\frac{2}{N} k_2 j + \phi_2 \right) + b : \quad (8)$$

In many cases with arbitrary amplitudes ($a_1; a_2$) and phases ($\phi_1; \phi_2$) were examined exhaustively; the wave numbers ($k_1; k_2$) were kept constant for each N tested. The results indicate that our conclusions are applicable in the more general case. In all our simulations, we found no regions with more than a single positive exponent (for N up to 60), including many cases with randomly chosen weights (i.e. arbitrary number of Fourier components).

Based on these results, we conjecture that the perceptron with a monotonic transfer function typically exhibits unstable behavior with a single positive Lyapunov exponent. Note that the bias term b , is crucial for producing chaotic behavior with monotonic transfer functions. Another important ingredient is the existence of a large enough phase, at least when the weights consist of a single Fourier component. It is possible that additional Fourier components are sufficient to generate unstable behavior (without large phase), however, larger phase significantly increases the number of unstable points.

Applying a non-monotonic transfer function gives rise to a different repertoire of properties in the parameter space (with respect to monotonic functions). One observes robust chaos, and the number of positive exponents can be larger than one. In the following analysis we use the sine as a representative function. At low gain values, quasi-periodic stationary solutions were found analytically, see [8]; in the following we focus on the region of high gain values where

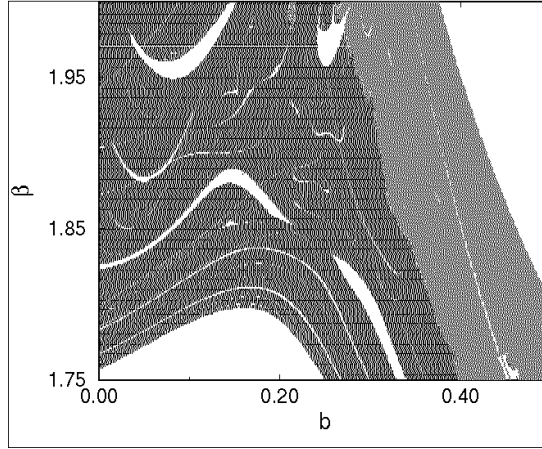


Fig. 3. { Analysis of a region in parameter space for a network with a sine transfer function and $N = 2$, where points that lead to chaotic trajectories are marked. The dark (gray) colors correspond to areas with one (two) positive exponent; the remaining space in this region leads asymptotically to stable attractors.

unstable behavior emerges. Note that in contrast to monotonic functions, unstable dynamics can be obtained with phase and bias equal to zero. Indeed, in the sequel we use $\phi = 0$; the parameter space remains two dimensional, (b, β) , as above.

Let us first describe the numerical analysis. A region in parameter space, for which the spectrum of Lyapunov exponents has been calculated, was sampled exhaustively in a resolution of 10^{-5} . Several random initial conditions were used for each vector in the parameter space to avoid possible isolated limit cycles. Figure 3 depicts such a region for $N = 2$, where vector points that lead to chaos are marked; vectors in white areas lead asymptotically to stable attractors. The dark area corresponds to a region with one positive exponent, while the gray area corresponds to a region with two positive exponents. A perusal in the figure reveals the following characteristics in the structure of the parameter space. The dark region (l.h.s. of the figure) contains extended (stable) windows (embedded white areas) associated with cycles of different length. The common feature of these windows is the fact that they are surrounded by unstable regions with one positive exponent. As we move to the right-hand side of the figure, a region with two positive exponents emerges; however, this type of trajectories is less interesting since the volume in phase space is expanding, hence, the bounded space is filled. The case $N > 2$ reveals another aspect in the structure of parameter space. There are regions for which we find more than two positive Lyapunov exponents. In such regions, we observed a robust chaos, namely, small changes of the parameters would not destroy the chaotic behavior. Figure 4 depicts the parameter space for $N = 9$ with weights prescribed by eq. 7 and $\phi = 0$. The dark area corresponds to a region with one or two positive exponents; the gray area corresponds to three positive exponents. In the gray area we observed a robust chaos with volume contracting attractors.

Let us now extend our analysis for large systems. Two questions come to the fore:

- (1) Can we find regions in which the chaotic dynamics is robust, and how frequent are they?
- (2) How does the attractor dimension relate to the control parameters?

We claim that the possibility of discovering regions with an increasing number of positive exponents, grows with N . This means that we have a natural parameter in the model that controls the structure of the chaos and the attractor dimension. In order to test this conjecture,

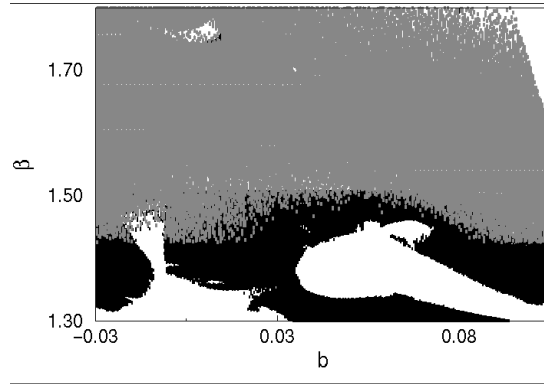


Fig. 4. Analysis of a region in parameter space for a network with a sine transfer function and $N = 9$. The dark area corresponds to one or two positive exponents; the gray area corresponds to three positive exponents. The remaining space in this region leads asymptotically to stable attractors.

we used a larger system, $N = 17$. For this analysis we used more complicated weights, consisting of two Fourier components with irrational phases and a bias term (eq. 8). The amplitudes and phases of the components were kept fixed, therefore, we have the same two dimensional parameter space, as before. The qualitative results reported below are insensitive to the exact values of the amplitudes and phases. A close inspection of the parameter space reveals the following regimes: First, the incommensurate regime which corresponds to the irrational phases of the weights. Above some value of the gain parameter (depending on the details of the weights) most of the space is associated with chaotic dynamics and the number of positive exponents grows with g (when the sum of the exponents becomes positive the dynamics is area expanding). In this regime, we observed a relatively monotonic growth of the attractor dimension. The estimation of the attractor dimension was done using the Kaplan-Yorke conjecture [14]. Figure 5(a) depicts the attractor dimension as a function of g for two fixed bias values. Clearly, the dimension grows monotonically. Figure 5(b) shows the sum of the exponents, $\sum_{i=1}^N \lambda_i$, in the same region of gain values. The sum grows monotonically, as expected, and saturates zero where the attractor dimension saturates the dimension of the system, N . Each point was averaged over 10 random initial conditions in order to check whether the same attractor is sampled. Indeed, the errors are less than 1% and typically much less, therefore, they are not presented. Note that there are cases, not shown in this figure, for which the line $b = \text{const}$ crosses a (stable) window; in these cases, the attractor dimension decreases and then continues to grow once the window is passed. Finally, we validated these results by estimating the attractor dimension from the time series generated by the network, and compared it to the estimation using the Kaplan-Yorke conjecture. The time series was recorded at the same time the spectrum of exponents was evaluated; the attractor dimension was calculated from the reconstructed phase space using the method of Correlation-Integral [15]. The results confirm our conjecture for the monotonic relation between the attractor dimension and g .

The major conclusion of this letter is that a NAR-perceptron model with non-monotonic transfer function can generate a stable chaotic attractor. The attractor dimension can be controlled by varying a parameter in the model. At this stage, we can not rule out the possibility that extremely tiny stable windows are situated in the vicinity of every chaotic point, however, this is very unlikely to be the case when the number of positive exponents is

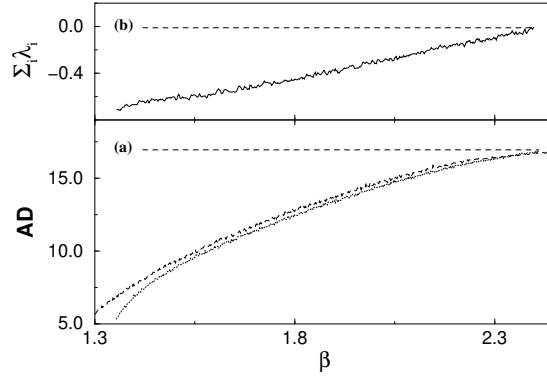


Fig. 5. (a) The attractor dimension (AD) as a function of the gain for a network with sine transfer function, $N = 17$, $\sigma = 0$, $b = 0$ - dashed line and $b = 0.05$ - long dashed line. The horizontal dashed line is at $AD = 17$. (b) The sum of Lyapunov exponents for $b = 0$. The horizontal dashed line is at $\sum_{i=1}^N \lambda_i = 0$.

much larger than the number of free parameters. In fact the larger N is, the less probable are the stable windows in these regions (see also [16]). Further analytical study of piecewise linear functions may clarify this issue. It is interesting to mention that Banerjee et. al. [17] showed a robust chaos in a simple 2D non-monotonic piecewise linear map.

Training a model to generate robust chaos seems to be limited to non-monotonic transfer functions, and may be of practical interest where reliable operation is necessary.

REFERENCES

- [1] Amit D. J., Modeling Brain Functions (NY: Cambridge university Press), 1989.
- [2] Babloyantz A., Nicolis C. and Salazar M., Phys. Rev. A 111, 152 (1985).
- [3] Sompolinsky H., Crisanti A. and Sommers H. J., Phys. Rev. Lett. 61, 259 (1988);
Laughton S. N. and Coolen A. C. C., J. Phys. A 27, 8011 (1994);
Kanter I., Phys. Rev. Lett. 77, 4844 (1996).
- [4] Tong H., Non-Linear Time Series (Oxford: Oxford university Press) (1990).
- [5] Siegelman H. T., Home B. G. and Giles C. L., IEEE Trans. Sys. Man and Cyber. 27, 208 (1997).
- [6] Moore C., Phys. Rev. Lett. 64, 2354 (1990).
- [7] Eisenstein E., Kanter I., Kessler D. A. and Kinzel W., Phys. Rev. Lett. 74, 6 (1995);
Schroder M. and Kinzel W., J. Phys. A 31, 2967 (1998);
Kanter I., Kessler D. A., Priel A. and Eisenstein E., Phys. Rev. Lett. 75, 2614 (1995).
- [8] Ein-Dor L. and Kanter I., Phys. Rev. E 57, 6564 (1998).
- [9] Priel A. and Kanter I., Phys. Rev. E 59, 3668 (1999).
- [10] Caroppo D., Mannarelli, Nardulli G. and Stramaglia S., Phys. Rev. E 60, 2186 (1999).
- [11] Yokoi C. S. O., Oliveira M. J. and Salinas S. R., Phys. Rev. Lett. 54, 163 (1985).
- [12] Moreira J. G. and Salinas S. R., J. Phys. A 20, 1621 (1987).
- [13] Wolf A., Swift J. B., Swinney H. L. and Vastano J. A., Physica D 16, 285 (1985).
- [14] Kaplan J. L. and Yorke J. A., Comm. Math. Phys. 67, 93 (1979).
- [15] Grassberger P. and Procaccia I., Physica D 9, 189 (1983).
- [16] Barreto E., Hunt B. R., Grebogi C. and Yorke J. A., Phys. Rev. Lett. 78, 4561 (1997).
- [17] Banerjee S., Yorke J. A. and Grebogi C., Phys. Rev. Lett. 80, 3049 (1998).